②

OFFICE OF NAVAL RESEARCH

Contract N00014-90-J-1828
R&D Code 413c024
Technical Report No. 61

Structural Rearrangements During Mesomorphic Phase Transitions in Poly{10-[(4-Cyano-4'-Biphenyl)oxy]Decanyl Vinyl Ether}

V. Tsukruk
Deutsches Kunststoff Institut
6100 Darmstart, Germany

V. Percec* and M. Lee
Department of Macromolecular Science
Case Western Reserve University
Cleveland, OH 44106-2699

Submitted for Publication

in

Polymer

March 27, 1992

SECURITY CLASSIFICATION OF THIS PAGE

REPORT DOCUMENTATION PAGE

1a REPORT SECURITY CLASSIFICATION Unclassified	1b RESTRICTIVE MARKINGS
2a SECURITY CLASSIFICATION AUTHORITY 2b DECLASSIFICATION / DOWNGRADING SCHEDULE	3 DISTRIBUTION / AVAILABILITY OF REPORT Available for distribution Distribution unlimited
4. PERFORMING ORGANIZATION REPORT NUMBER(S) Technical Report No. 61	5 MONITORING ORGANIZATION REPORT NUMBER(S)

6a NAME OF PERFORMING ORGANIZATION Case Western Reserve University	6b OFFICE SYMBOL *(If applicable)* 4B566	7a NAME OF MONITORING ORGANIZATION ONR
6c ADDRESS *(City, State, and ZIP Code)* 2040 Adelbert Road Cleveland, OH 44106		7b ADDRESS *(City, State, and ZIP Code)* Office of Naval Research Arlington, VA 22217
8a NAME OF FUNDING / SPONSORING ORGANIZATION ONR	8b OFFICE SYMBOL *(If applicable)*	9 PROCUREMENT INSTRUMENT IDENTIFICATION NUMBER

8c ADDRESS *(City, State, and ZIP Code)* Office of Naval Research 800 N. Quincy Arlington, VA 22217	10 SOURCE OF FUNDING NUMBERS			
	PROGRAM ELEMENT NO. N00014-89	PROJECT NO. J-1828	TASK NO 413c024	WORK UNIT ACCESSION NO

11 TITLE *(Include Security Classification)*
Structural Rearrangements During Mesomorphic Phase Transitions in Poly{10-[(4-Cyano-4'-Biphenyl)oxy]Decanyl Vinyl Ether}

12. PERSONAL AUTHOR(S) V. Tsukruk, V. Percec* and M. Lee

13a TYPE OF REPORT Preprint	13b TIME COVERED FROM ______ TO ______	14 DATE OF REPORT *(Year, Month, Day)* March 27, 1992	15. PAGE COUNT

16. SUPPLEMENTARY NOTATION
Polymer

17. COSATI CODES			18 SUBJECT TERMS *(Continue on reverse if necessary and identify by block number)*
FIELD	GROUP	SUB-GROUP	

19. ABSTRACT *(Continue on reverse if necessary and identify by block number)*

The side chain liquid crystalline poly{10-[(4-cyano-4'-biphenyl)oxy]decanyl vinyl ether} exhibits two different smectic phase: at low temperature an ordered smectic E phase with orthorhombic intralayer packing of the mesogenic groups, and at high temperatures a common disordered smectic A phase. In both phases a double-layered longitudinal packing of the macromolecular fragments with a thickness of 6.6 -7 nm and overlapping of the slightly tilted mesogenic groups is realized. During the phase transition from the smectic E to the smectic A a melting of the intralayered packing occurs which leads also to the slight changes of the thickness of the smectic layers as a result of the conformational disordering of the side chains. A smectic A-like structure could be freezed in the glassy state by quick cooling. The development of the ordered smectic E phase as a result of annealing at temperatures higher than Tg is a very slow process since it requires the formation of the ordered intralayered orthorhombic packing of mesogenic groups.

20. DISTRIBUTION / AVAILABILITY OF ABSTRACT ☒ UNCLASSIFIED/UNLIMITED ☐ SAME AS RPT. ☐ DTIC USERS	21. ABSTRACT SECURITY CLASSIFICATION unclassified/unlimited	
22a NAME OF RESPONSIBLE INDIVIDUAL Virgil Percec	22b. TELEPHONE *(Include Area Code)* (216) 368-4242	22c. OFFICE SYMBOL

DD FORM 1473, 84 MAR 83 APR edition may be used until exhausted.
All other editions are obsolete.
SECURITY CLASSIFICATION OF THIS PAGE

STRUCTURAL REARRANGEMENTS DURING MESOMORPHIC PHASE TRANSITIONS IN POLY{10-[4-CYANO-4'-BIPHENYL)OXY]DECANYL VINYL ETHER

V. Tsukruk
Deutsches Kunststoff Institut
6100 Darmstadt, Germany

Virgil Percec* and Myongsoo Lee
Department of Macromolecular Science
Case Western Reserve University
Cleveland, OH 44106, U. S. A.

* To whom all correspondence should be addressed.

INTRODUCTION

In recent years interest in poly(vinyl ether)s containing mesogenic side groups increased mainly because they can be synthesized by a living polymerization recation.[1-4] Our investigations on the polymerization of mesogenic vinyl ethers were performed with the initiating system $CF_3SO_3H/(CH_3)_2S$ which leads to a living polymerization at 0^oC in methylene chloride.[5] So far, we have elucidated the influence of molecular weight on the phase transitions of poly{ω-[4-cyano-4'-biphenyl)oxy]alkyl vinyl ether}s with flexible spacers containing from 2 to 11 methylenic units,[6] and of some other mesogenic vinyl ethers.[7] These results have demonstrated that the nature and the number of mesophases exhibited by side chain liquid crystallize polymers are most of the time molecular weight dependent. In addition, living copolymerization experiments were used to tailor make copolymers exhibiting nematic, smectic A and reentrant nematic phases.[6-8]

Poly{10-[(4-cyano-4'-biphenyl)oxy]decanyl vinyl ether}[poly(6-10)] with degrees of polymerization higher than 16 exhibits an unidentified smectic mesophase followed by an enantiotropic smectic A mesophase.[6] In order to provide a complete elucidation of the phase behavior of poly(6-10), we must understand the structural arrangement of the polymer side groups in its different liquid crystalline states.

The goal of this paper is to elucidate during the phase behavior and the structural rearrangements of the layer and intralayer ordering during the phase transitions between the liquid crystalline states of poly(6-10) with a degree of polymerization of 19.

EXPERIMENTAL

Materials

The synthesis of 10-[(4-cyano-4'-biphenyl)oxy]decanyl vinyl ether (6-10), its living cationic polymerization initiated with $CF_3SO_3H/S(CH_3)_2$ in CH_2Cl_2 at 0^0C and the characterization of the resulted polymers were presented in a previous publication from our laboratory[6]. Table 1 summerizes the polymerization results. The structure of this polymer is shown in Scheme I.

Techniques

Differential scanning calorimetry measurements were performed on a Perkin-Elmer DSC-4 instrument equipped with a TADS data station Model 3600. Heating and cooling rates were 20°C/min. First order transitions were recorded at the maximum of the endothermic or exodermic peaks. A Carl-Zeiss optical polarized microscope (magnification: 100x) equipped with a Mettler FP 82 hot stage and a Mettler FP 800 central processor was used to observe the thermal transitions and to analyze the anisotropic textures. Before the X-ray experiments, the polymer sample was heated to isotropic temperature then was cooled very slow to the liquid crystalline state during 10 hours and then was annealed at 35°C during 1 day . The oriented sample was obtained by very slow step-by-step cooling from the isotropic state to 35°C during 1 week in a magnetic field of 1 T. X-ray wide-angle scattering (WAXS) curves were recorded on a Siemens D-500 difractometer. Small-angle X-ray scattering (SAXS) curves were obtained on a compact Kratky camera with positional detector. X-ray photo-patterns on oriented sample were obtained on flat cameras with different distances from the sample-film. In all cases a Ni-filtered CuKα radiation was used. Before the measurements the sample was kept at the desired temperature for at least 1 hour. The accuracy of the temperature of the thermostated sample was about ±1°

The analysis of the SAXS data was made by using the programs FFSAXS. This program includes the smoothing of the data by cubic polynoms, the substraction of the background and calculation of the one-dimensional correlation functions G(x) by cosine-Fourier transform of the Lorenz corrected data. The analysis of the WAXS data was performed by using the program FIT which includes the smoothing of the data by splines, the substraction of the diffuse background and the fit the observed maxima by various scattering functions. Additional experimental details on the characterization by WAXS and SAXS and on the processing of the results were presented elsewhere.[9]

The spatial arrangement and the geometric sizes of the molecular fragments was analyzed for two conjugated monomeric units by the modeling program INSIGHT and the most favourable conformation was calculated by using the program DISCOVER.

RESULTS AND DISCUSSIONS

A poly(6-10) with degree of polymerization equal to 19 and Mw/Mn=1.14 was used in all investigations. The DSC thermograms of this polymer are shown in Figure 1. Both in the heating and cooling scans, the low temperature unidentified smectic phase is separated from the high temperature smectic A phase by a first order transition (Figure 1). On the optical polarized microscope, the high temperature mesophase exhibits a focal conic texture which is characteristic to a smectic A phase, while the low temperature phase shows a broken focal conic texture. To elucidate the possible structure and the nature of mesomorphic transition between these two phases, first the structure of the low-temperature phase and the parameters of structural packing in the smectic A phase were determined. Latter we will discuss the corresponding structural rearrangements during this phase transition.

Low Temperature Smectic Phase

On the WAXS curves obtained at low temperatures two different sets of scattering peaks were observed: two very strong sharp peaks at 2.6° and 5.2° overlapped with a diffuse halo at 6-7° and a modulated broad peak consisting of some overlapped maxima in the range of 20° (Figure 2).On the corresponding SAXS curves these two sharp peaks are visible more clear and an additional diffuse halo around 1° is also detected (Figure 3). The d-spacings of these X-ray data were calculated according to the Braggs law and are presented in Table 2.

In the X-ray patterns of the polymer oriented in the magnetic field one can observe a meridional arrangement of the SAXS reflexions while all three sharp WAXS reflexions are concentrated in the very spreaded equatorial arcs (Figures 2 and 3).

The presence on the WAXS curves of three overlapped peaks points out to the formation of ordered intralayered packing of the mesogenic groups in low-temperature smectic phase. The WAXS maximum was splitted in three sharp maxima of a Lorentz shape with half-widths of about 2° (Table 2, Figure 4). The absolute values of the intralayered correlation lengths $\xi_\perp$ are in the range of 1.4 nm. This value is much higher than the typical values for disordered smectic phases (0.3-0.6 nm) but slightly lower than the typical ones observed for an ordered smectic phase in side chain liquid crystalline polymers[9-11]. The correlations in the intralayered ordering ($L \approx 3\text{-}4\ \xi$) are expanded to 5-6 nm. Thus the regions with ordered intralayered packing include more than one hundred mesogenic groups which corresponds to the existence of a two dimensional lattice. As judged from the X-ray patterns, the mesogenic side groups are oriented along the direction of the magnetic field (Figures 2 and 3) and are arranged into layers orthogonally to the smectic plane.

The presence in WAXS angular region of the three sharp peaks orthogonally arranged according to the SAXS layered reflections is typical for a smectic E phase with orthorombic symmetry of the two dimensional lattice[11,12]. The position of all reflexes are indexed quite well as the 020, 100 and 110 reflections of the orthorombic unit cell with the parameters: a=0.4 nm, b=0.914 nm and $c \approx 3.36$ nm. Such a lattice is formed by the herringbone packed mesogenic groups with two different orientations of their short axes in the layered planes.[10,11] Thus from the analysis of all avalable data we can conclude that the phase from the low temperature is a smectic E phase with two-dimensional intralayered packing of orthorombic symmetry.[12,13]

Let us consider the perfection of the one-dimensional ordering and the possible models of longitudinal packing of the macromolecular fragments in this phase. In order to characterize the perfection of the one-dimensional order we calculated the one-dimensional correlation function G(x) (Figure 5). The G(x) is common for lammellar phases of damping oscillations with a main period of 6.6 nm. The value of the longitudinal correlation length ξ calculated from G(x)[9] is equal to 35 nm. This value is also typical for smectic ordered phases of side-chain polymers with a high concetration of defects formed by the coil-like flexible backbones.[9,10]

As deduced from the highest intensity of the second maximum of G(x), the main period of density distribution which corresponds to the thickness of the layers is equal to 6.6nm. Such a periodicity fits quite well to the common double-layered structures of the cyano-containing mesogenic groups with partial overlapping of the side fragments (Figure 6). As judged from conformational calculations, the cyano biphenyl mesogenic groups are arranged at definite angle according to the orthogonal direction of the methylene spacer as shown in Figure 4, and in the framework of the proposed packing they are fully overlapped. *The main periodicity of 6.6 nm is determined* by the distance between the backbones arranged in the same plane (Figure 6). This distance is twice higher than the d-spacing calculated from the position of the first SAXS peak (Table 2). We also observe an additional maximum at 3.3 nm whch points out to the existence of an additional half-period density wave. This situation is very similar to that discussed in details for other ordered side-chain smectic polymers [9-11] and demonstrates the existence of an additional peridiocity normal to the smectic planes between dense packed mesogenic groups of the neighboring molecules (Figure 7). As it is well known for layered structures, the existence of such additional half-periods in density distribution leads to the extinction of the odd orders of reflections[12,13]. Thus for the layered packing of the polymer studied, the first order of the reflection with d=6.6nm should be extincted and the observed SAXS peaks are 2 and 4 orders of reflections of the proposed double-layed packing. Thus from this discussion we can conclude that the low-temperature phase in this polymer is a smectic E phase with orthorombic intralayered order and double-layered longitudinal packing and with overlapped cyanobiphenyl mesogenic groups in the side chains.

High-Temperature Smectic Phase

As was mentioned above the high-temperature phase in this polymer is most probably the common disordered smectic A phase.[12] From the obtained data we can conclude that the well defined layered structure is maintained in this phase only with a slightly changed periodicity and liquid-like quasi-hexagonal ordering into layers (Figure 2,3). As a result of the two dimensional melting of the intralayered lattice only a short-range order is detected in this phase. The short-range order in the intralayered packing of the mesogenic groups is expanded only on $L=1\text{-}2$ nm which is typical for a smectic A mesophase. The thickness of layers of 7 nm is only slightly higher as compared to the initial double-layered packing. The perfection of the one-dimensional order in the smectic A *phase is much higher* as compared to the ordered smectic E phase. The value of the longitudinal correlation lengths ξ is resolution limited and is not lower than 100 nm (Figure 5).

Thus the high temperature phase in this liquid crystalline polymer is a common disordered smectic A phase with interdigitated double-layered packing, long range longitudinal ordering and short-range order into layers. It is obvious from the comparison of the structural data of these two phases that during the phase transformation smectic E-smectic A, different changes of the structural ordering are observed such as: melting of the intralayered ordering, change of the thickness of the layered packing and the disappearance of the SAXS diffused halo. All these structural changes will be discussed in the next subchapter.

Structural Changes Observed During the Cycle: Heating-Cooling-Annealing

Intralayered Packing

The heating of the polymer up to T_1 leads only to minor changes of the WAXS scattering while an increase of temperature to above T_1 provides the appearance of the diffuse halo (Figure 2). These changes of WAXS scattering occur in a very narrow temperature interval (2-4°) near T_1 and correspond to the so called two dimensional-melting of the intralayer packing during the transition from the ordered to the disordered smectic phase.[9,10] The orthorombic symmetry of the intralayer packing of the smectic E phase is broken and a common quasi-hexagonal short-range order is formed. The corresponding intralayer correlation length drops abruptly about 3-4 times (from 1.4 to 0.4 nm).

During the cooling of the high-temperature phase, the phase transformation occurs at T_1=37° (according to the DSC data with rate of 20 °C/min). But on the WAXS curve this phase transition occurs during 2 hours at room temperature. After the sample was slowly cooled at 35 °C for 10 hr the initial overlapped sharp peaks are restored and the ordered intralayered ordering which characterizes the smectic E phase is formed. Consequently, as a result of cooling from smectic A state in a glassy state we have generated a metastable structure with liquid-like intralayered order coexisting with the partially transformed ordered phase. This metastable structure could be transformed into the initial ordered smectic E state by prolonged annealing at temperatures higher than the glass transition temperature. This observation is also confirmed by the observed changes of DSC traces for samples with different thermal prehistory.

Layer Packing

During the transformation from smectic E to smectic A phase an increase of the intensity of the SAXS maximum and of the corresponding d-spacings as well as the disappearance of the diffuse halo from around 1° are observed simultaneously (Figure 3). All these changes occur very sharply in a narrow interval of 2°C width, i.e., from 54 to 56 °C (see for example Figure 8). The longitudinal correlations increase sharply also after the transition from the smectic E into the smectic A phase (Figure 5). The increase of the thickness of the smectic layers during the melting of the intralayered packing can be explained very easily by the free rotation of the mesogenic groups in the smectic A phase. As can be seen from Figure 5 the introduction of only one gauche-conformer into the side chain, leads to the arrangement of the biphenyl moieties along the overall direction of the side chains. Correspondingly the projection of one side chain normal to the smectic plane increases with 0.15-0.2 nm. This leads to an increase of the overall thickness of the initial double-layered packing of 0.3-0.4 nm which corresponds to the observed value (Table 2).

The SAXS curve of the polymer cooled to room temperature from the isotropic state differs from the initial one. The sharp maximum shifts to the higher angles and the diffuse one from around 1° is not restored (Figure 8). After annealing at 35 °C for two hours the sharp peak is shifted to the lower angles and the diffuse maximum at 1° appears. A longer annealing time of about 1 day leads to a full restoration of the initial curve of the annealed sample (Figure 9, Table 2). Tne longitudinal correlations are lowered very strongly during cooling and the hight of the second maximum on G(x) increases (Figure 5b). All these data are the result of the quick cooling of the polymer from the isotropic state into the glassy state with a freezing of the smectic A-like structure containing the liquid-like intralayer ordering. The development of the ordered smectic E phase at a temperature higher than Tg is a very slow process and the formation of the orthorombic lattice in the intralayer packing of the mesogenic groups with conformational changes in side groups is accompanied by the appropriated changes of the layer ordering.

CONCLUSIONS

The side chain liquid crystalline polymer, poly(6-10), exhibits two different smectic phases: at low temperature an ordered smectic E phase with orthorombic intralayer packing of the mesogenic groups, and at high temperatures a common disordered smectic A phase. In both phases a double-layered longitudinal packing of the macromolecular fragments with a thickness of 6.6 nm-7 nm and overlapping of the slightly tilted mesogenic groups is realized. During the phase transition from the smectic E to the smectic A a melting of the intralayered packing occurs which leads also to the slight changes of the thickness of the smectic layers as a result of the conformational disordering of the side chains. A smectic A-like structure could be freezed in the glassy state by quick cooling. The development of the ordered smectic E phase as a result of annealing at temperatures higher than Tg is a very slow process since it requires the formation of the ordered intralayered orthorombic packing of mesogenic groups.

ACKNOWLEDGMENT

Financial support from the Office of Naval Research is gratefully acknowledged.

REFERENCES

1. (a) Rodriguez-Parada, J. M. and Percec, V., *J. Polym. Sci.: Part A: Polym. Chem.*, 1986, **24**, 1363; (b) Percec, V. and Tomazos, D., *Polym. Bull.*, 1987, **18**, 239
2. (a) Sagane, T. and Lenz, R. W., *Polym. J.*, 1988, **20**, 923; (b) Sagane, T. and Lenz, R. W., *Polymer*, 1989, **30**, 2269; (c) Sagane, T. and Lenz, R. W., *Macromolecules* , 1989, **22**, 3763
3. Kostromin, S. G.; Cuong, N. G.; Garina, E. S. and Shibaev, V. P., *Mol. Cryst. Liq. Cryst.*, 1990, **193**, 77
4. Heroguez, V., Deffieux, A. and Fontanille, M., *Makromol. Chem., Makromol. Symp.*, 1990, 32, 199; Heroguez, V., Schappacher, M., Papon, E. and Deffieux, A., *Polym. Bull.*, 1991, **25**, 307
5. Cho, C. G., Feit, B. A. and Webster, W. A., *Macromolecules*, 1990, **23**, 1918; Lin, C. H. and Matyjaszewsky, *Polym. Prepr. Am. Chem. Soc. Div. Polym. Chem.*, 1990, **31(1)**, 599

6. (a) Percec, V.; Lee, M. and Jonsson, H., *J. Polym. Sci.: Part A: Polym. Chem.*, 1991, **29**, 327; (b)Percec, V. and Lee, M., *J. Macromol. Sci.-Chem.*, 1991, A 28, 651; (c) Percec, V. and Lee, M., *Macromolecules*, 1991, **24**, 1017; (d) Percec, V. and Lee, M., *Macromolecules*, 1991, **24**, 2780; (e) Percec, V.; Lee, M. and Ackerman, C., *Polymer*, in press.17. Kostromin, S. G.; Cuong, N. G.; Garina, E. S. and Shibaev, V. P., 1990, *Mol. Cryst. Liq. Cryst.*, **193**, 77

7. (a) Percec, V.; Gomes, A. and Lee, M., 1991, *J. Polym. Sci.: Part A: Polym. Chem. Ed.*, **29**, 1615; (b) Percec, V., Wang, C. H. and Lee, M., *Polym. Bull.*, 1991, **26**, 15; (c) Percec, Zheng, Q. and Lee, M., *J. Mater. Chem.*, 1991, **1**, 611

8. (a) Percec, V. and Lee, M., *Polym. Bull.*, 1991, **25**, 123; (b) Percec, V. and Lee, M, *Polym. Bull.*, 1991, **25**, 131; (c) Percec, V. and Lee, M, *Macromolecules*, 1991, **24**, 4963; (d) Percec, V. and Lee, M., *Polymer*, 1991, **32**, 2862; (e) Percec, V. and Lee, M., *J. Mater. Chem.*, 1991, **1**, 1007

9. Tsukruk, V., Shilov, V. and Lipatov, Y., Macromolecules, 1986, 19, 1308

10. (a) Tsukruk, V., Shilov, V. and Lipatov, Y., *Acta Polym.*, 1985, **36**, 403; (b) Lipatov, Y., Tsukruk, V. and Shilov, V.,*J. Macromol. Sci., Macromol. Chem. Phys.*, 1984, C24, 173.

11. Noel, C., in "Side Chain Liquid Crystal Polymers" McArdle, C. B., Eds., Chapman and Hall, New York, 1989, p. 159

12. Hefrich, W., *J. Phys. (Paris) Coll.*, 1979, **40**, C3

13. Gray, G. W. and Goodby, G. W., "Smectic Liquid Crystals, Leonard Hill, Glasgow, 1984

FIGURE AND SCHEME CAPTIONS

Scheme I. The structure of poly{10-[(4-cyano-4'-biphenyl)oxy]decanyl vinyl ether} poly(6-10)

Figure 1. Heating and cooling DSC traces (20 °C/min) of poly(6-10) with DP=19: A) first heating scan; B) second and subsequent heating scan; C) first and subsequent cooling scan.

Figure 2. Wide-angle-X-ray scattering curves of poly(6-10) at different temperatures.

Figure 3. Small angle X-ray scattering curves of poly(6-10) at different temperatures.

Figure 4. Split of the WAXS for the smectic E phase of poly(6-10) by Lorentz profiles.

Figure 5. One-dimensional correlation functions G(x) of poly(6-10) in the smectic E and smectic A phases (a) and in smectic E phase after cooling and annealing (b).

Figure 6. Molecular models of the liquid crystalline poly(6-10): (a) model of double-layered packing with overlapping of the mesogenic groups (main periodicity and half periodicity are shown), (b) possible changes of the arrangement of the biphenyl mesogenic groups as a result of tortional rotation.

Figure 7. Wide-angle X-ray scattering curves of poly(6-10) at 35°C after cooling and annealing during 1 day.

Figure 8. The dependence of d-spacing of poly(6-10) on temperature.

Figure 9. Small-angle X-ray scattering curves of poly(6-10) obtained during annealing.

Table 1; Cationic Polymerization of 6-10 and Characterization of the Resulting Polymer

$[M]_o/[I]_o$	$Mn \times 10^{-3}$	Mw/Mn (GPC)	DP	phase transitions (°C) and corresponding enthalpy changes (kcal/mru)	
				heating	cooling
20	7.3	1.14	19.0	g 15.5 k 55.0 (2.39) s_A 153.7 (0.76) i g 16.2 s_X 44.9 (0.68) s_A 152.9 (0.74) i	i 147.3 (0.72) s_A 37.4 (0.80) s_X 11.8 g

Table 2. Structural characteristic of poly(6-10)

	Temperature	d-spacings (nm)								
	(°C)	1	2	3	4	5	6	7	$\xi_{\parallel}$	$\xi_{\perp}$
LC I state										
	25, cooled		3.17	1.59					45	
	25, annealed 2 hr	8.8 w	3.33	1.63	1.3 w	0.454				0.5
	25, annealed 1 day	8.8 w	3.36	1.65	1.3 w	0.457	0.41	0.374	35	1.4
LC II state										
	59		3.52	1.76	1.2 w	0.45			>100	0.4

the accuracy of d-spacings in SAXS region is 0.5 nm for sharp peaks and 0.1 nm for weak ones; in WAXS region the accuracy is 0.005 nm; w-weak intensity

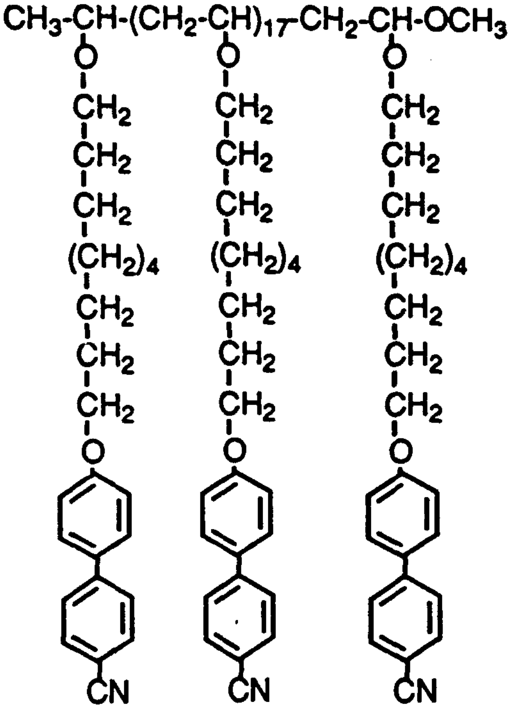

Scheme I

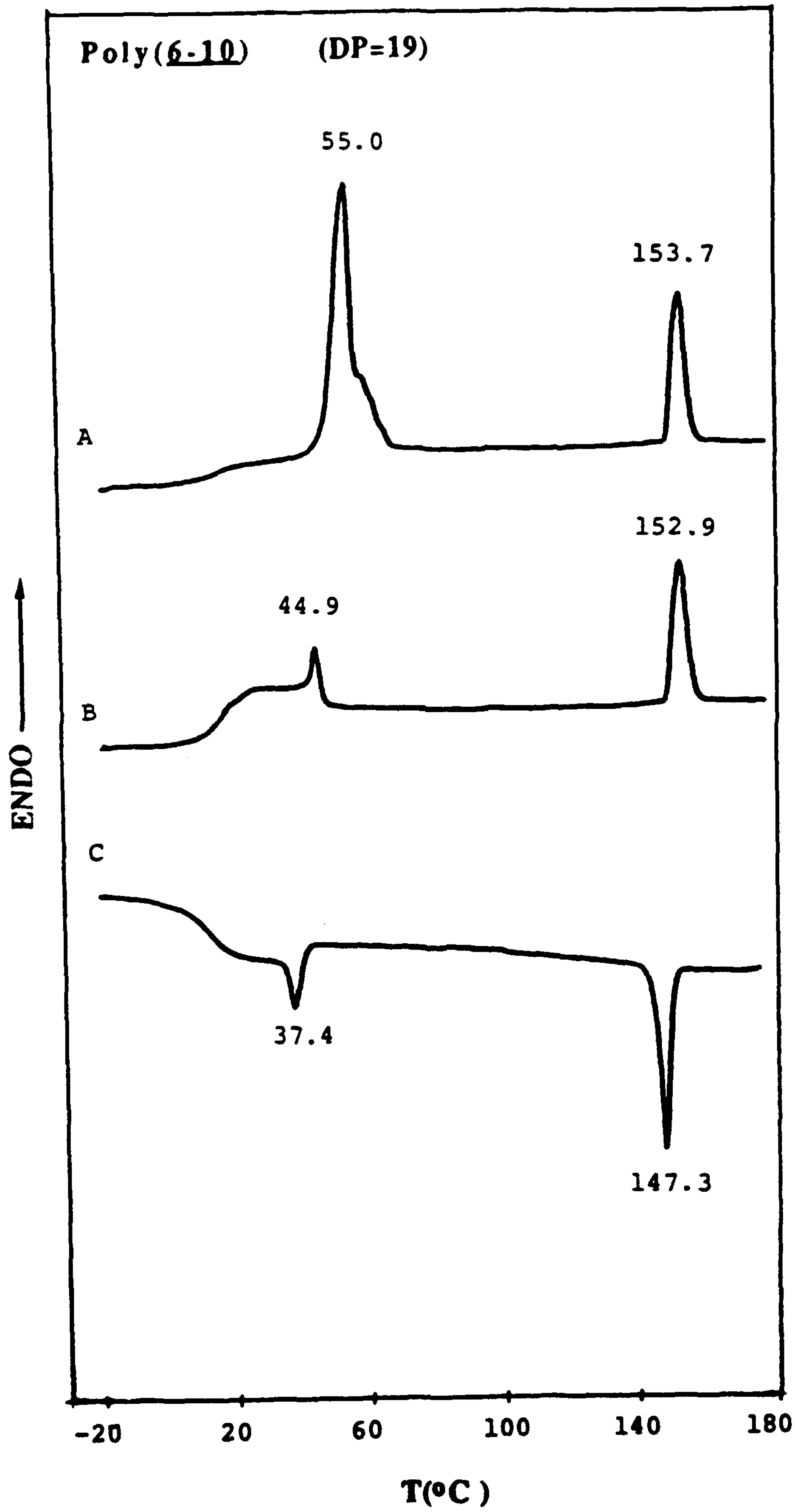
Poly(6-10) (DP=19)
55.0
153.7
A
152.9
44.9
B
ENDO
C
37.4
147.3
-20
20
60
100
140
180
T(°C)

Figure 1

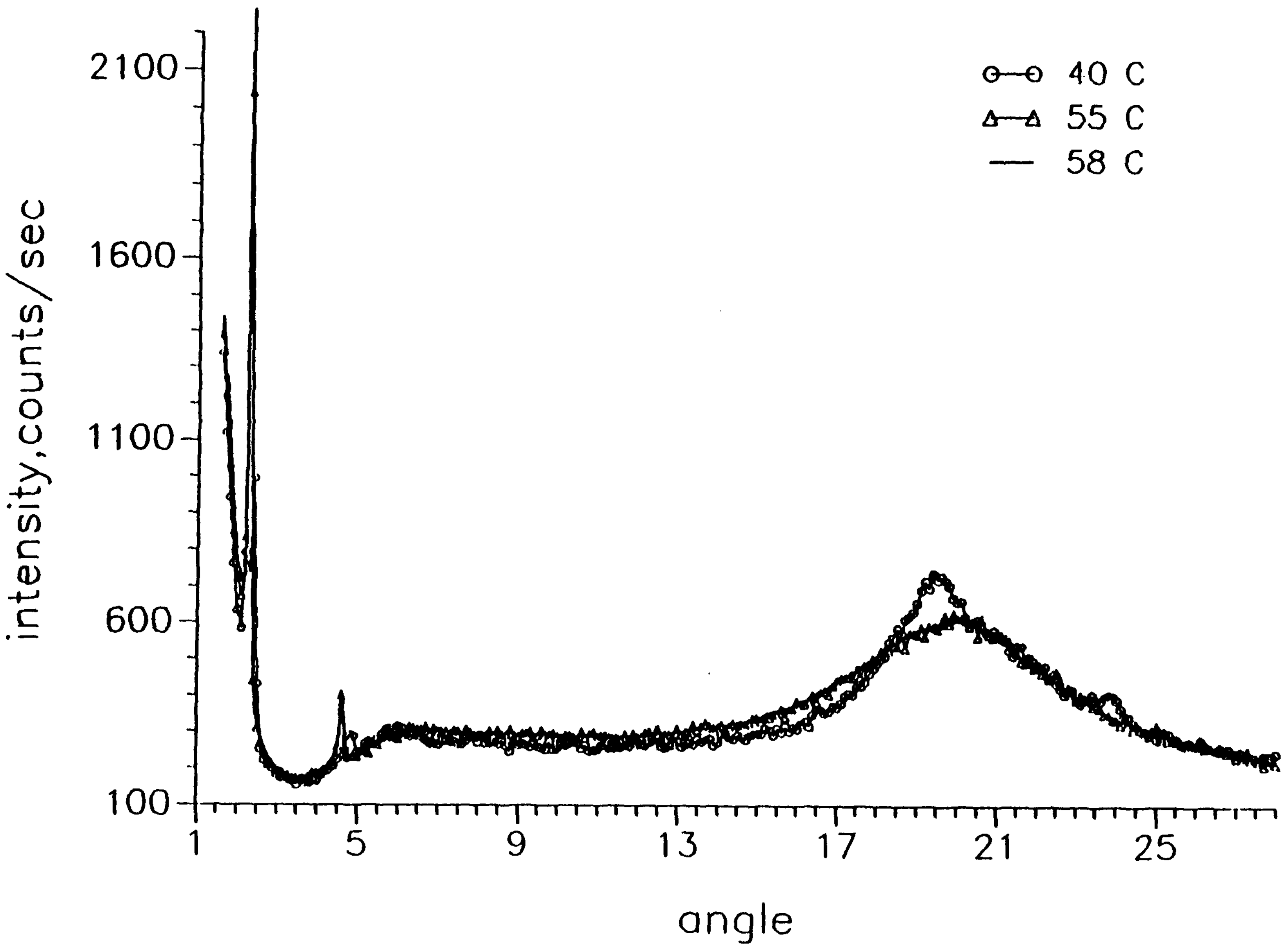

40 C
55 C
58 C
intensity,counts/sec
2100
1600
1100
600
100
1
5
9
13
17
21
25
angle

Figure 2

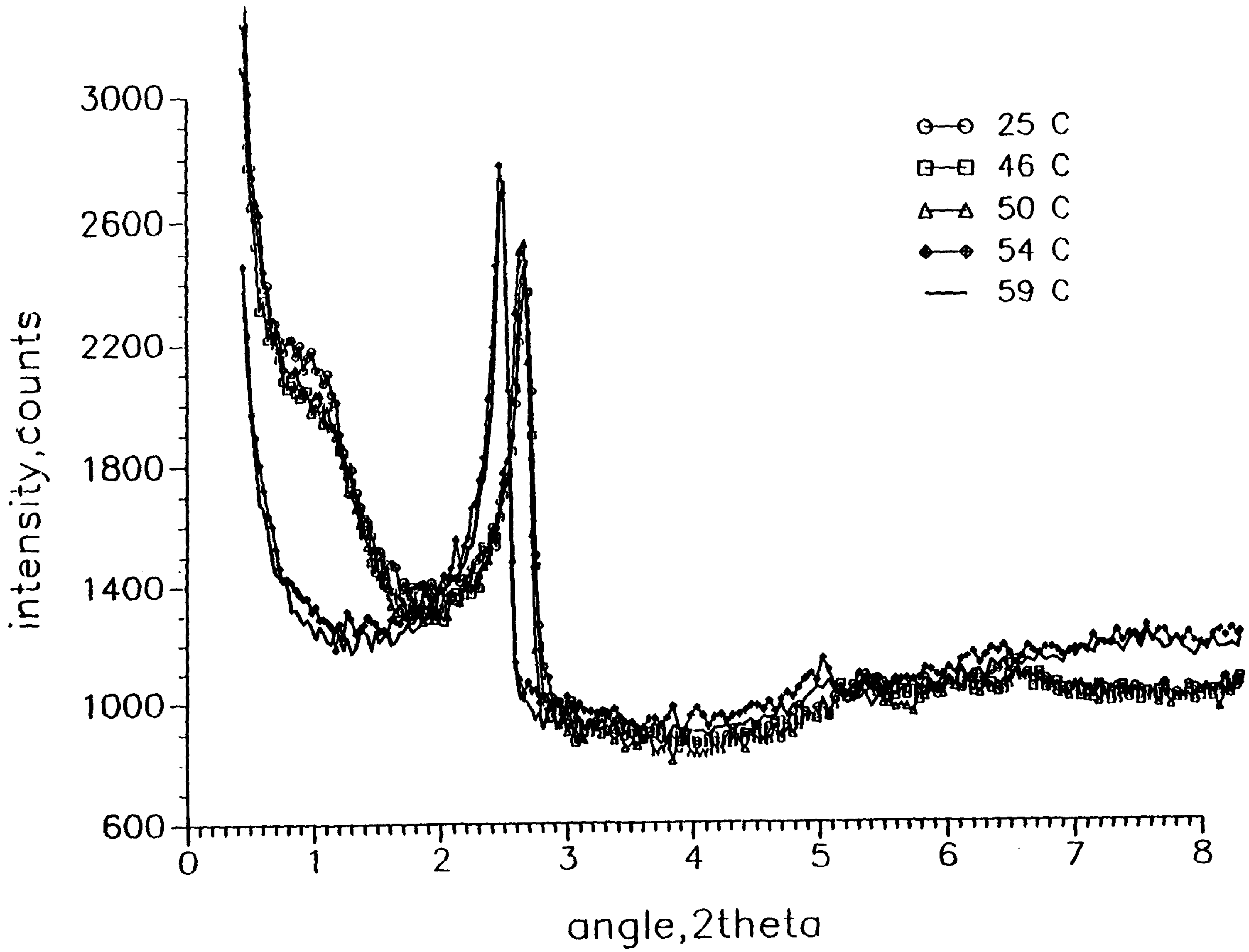
3000
2600
2200
1800
1400
1000
600
intensity,counts
0
1
2
3
4
5
6
7
8
angle,2theta
25 C
46 C
50 C
54 C
59 C

Figure 3

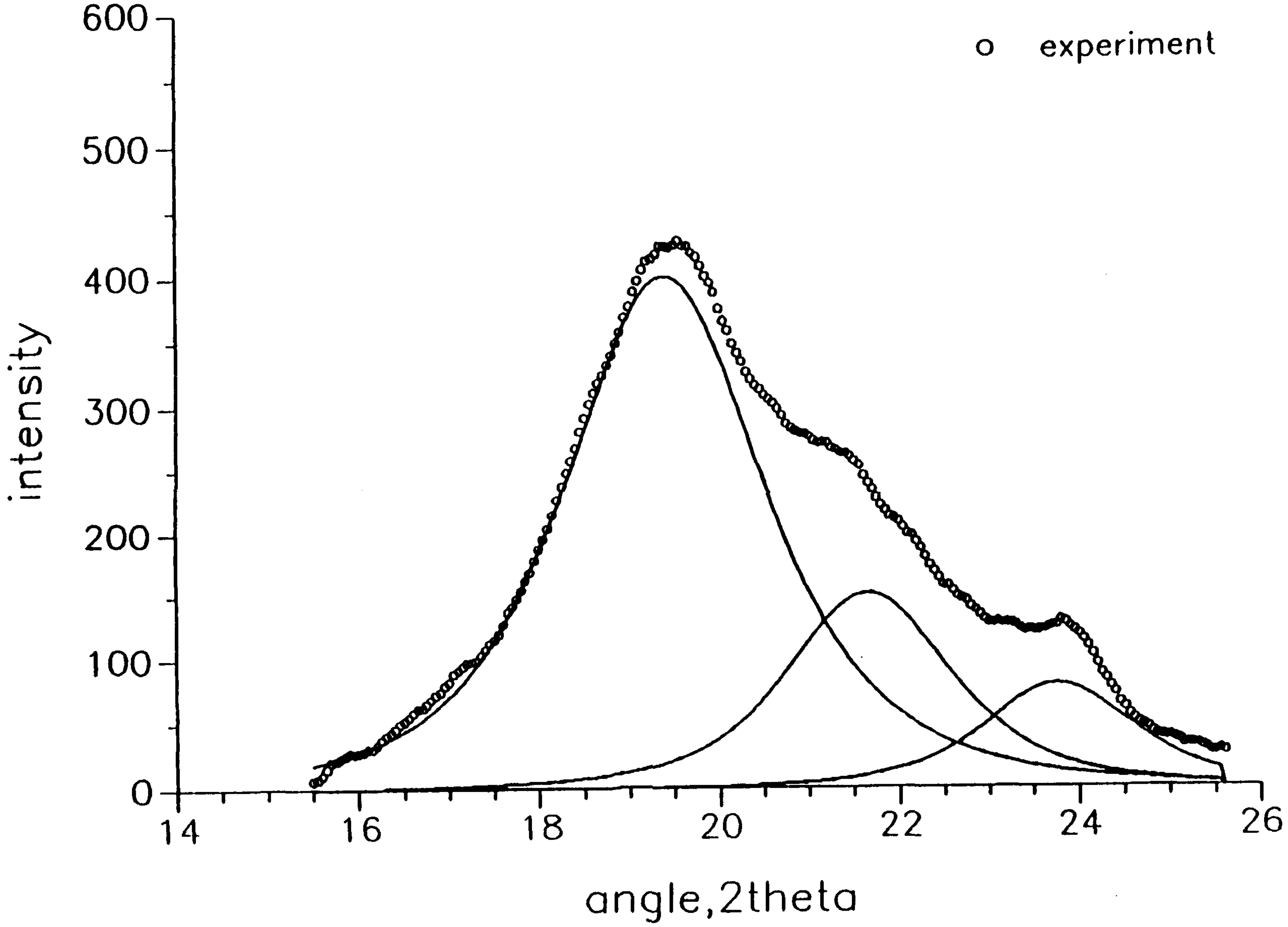
600
500
400
300
200
100
0
intensity
14
16
18
20
22
24
26
angle,2theta
o experiment

Figure 4

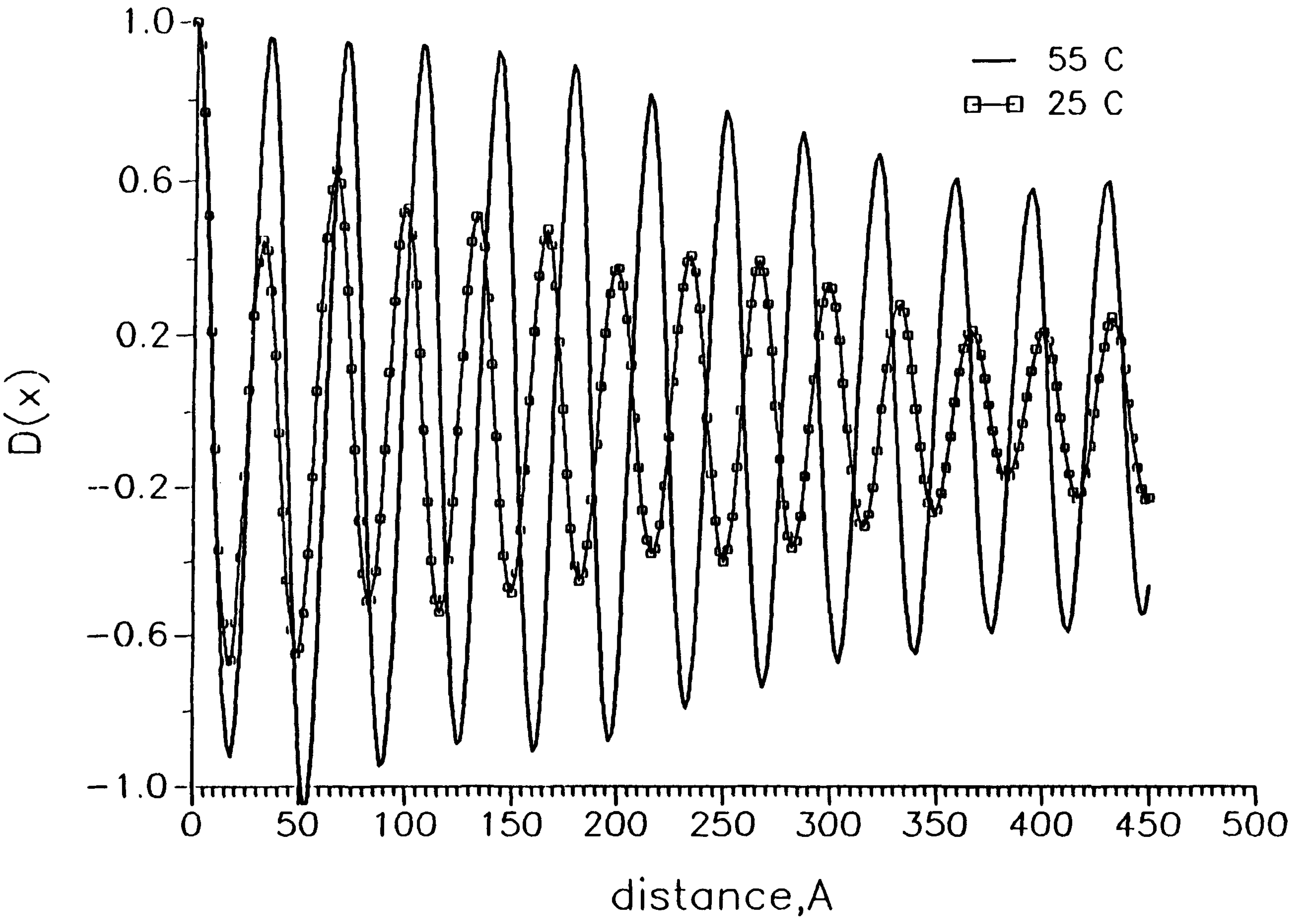
1.0
0.6
0.2
-0.2
-0.6
-1.0
D(x)
0
50
100
150
200
250
300
350
400
450
500
distance,A
55 C
25 C

Figure 5 a

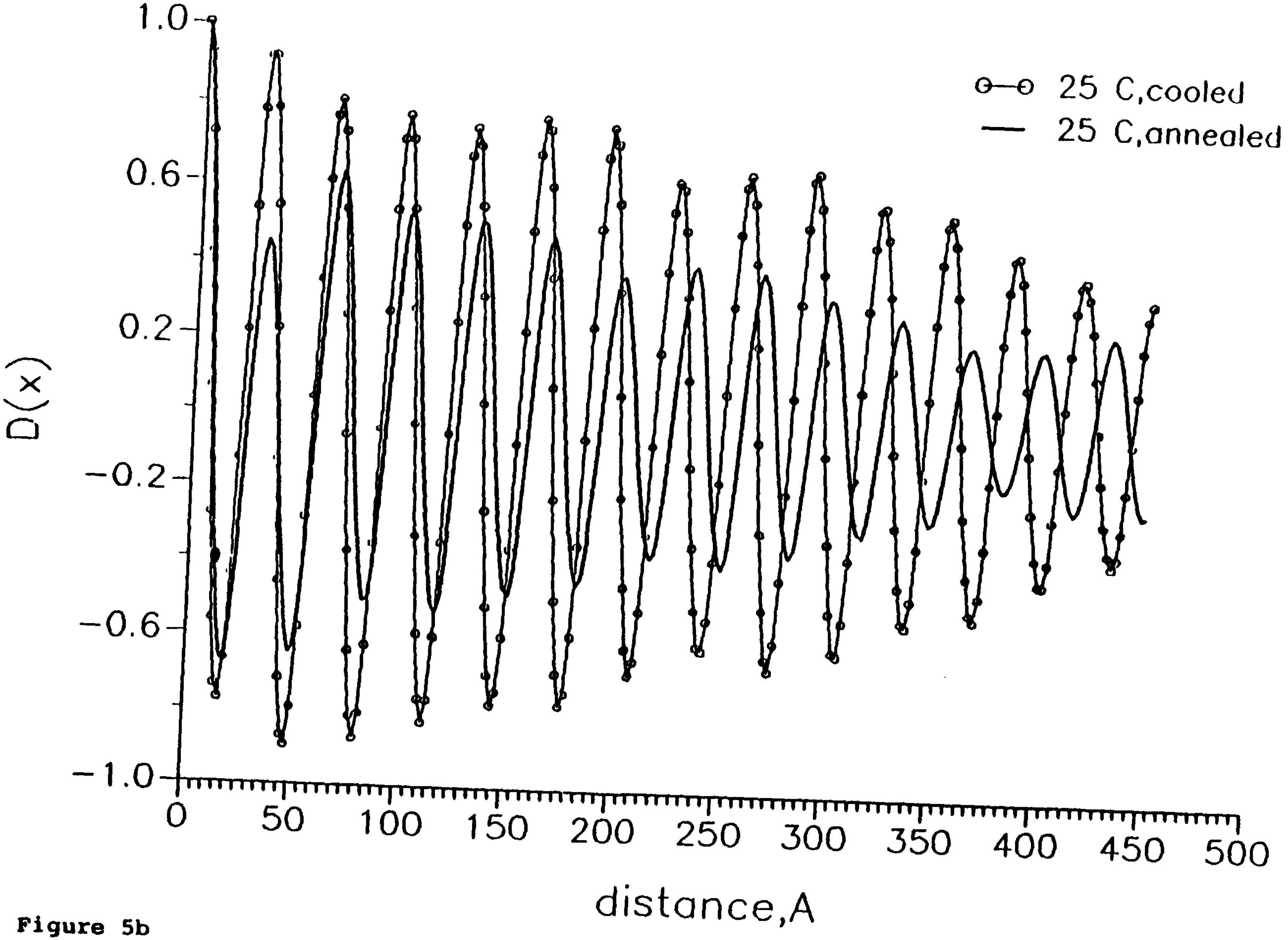
1.0
0.6
0.2
−0.2
−0.6
−1.0
D(x)
0
50
100
150
200
250
300
350
400
450
500
distance,A
25 C,cooled
25 C,annealed

Figure 5b

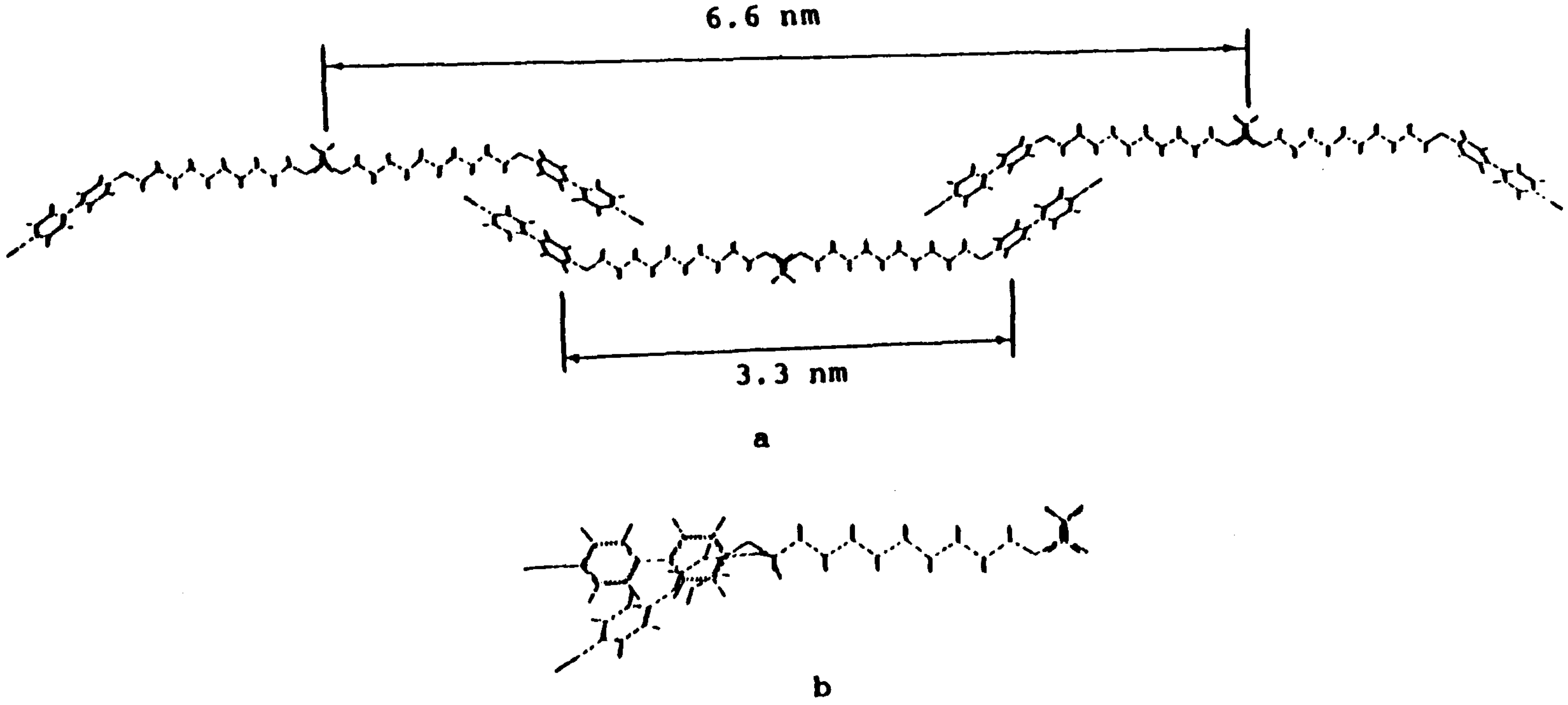

Figure 6

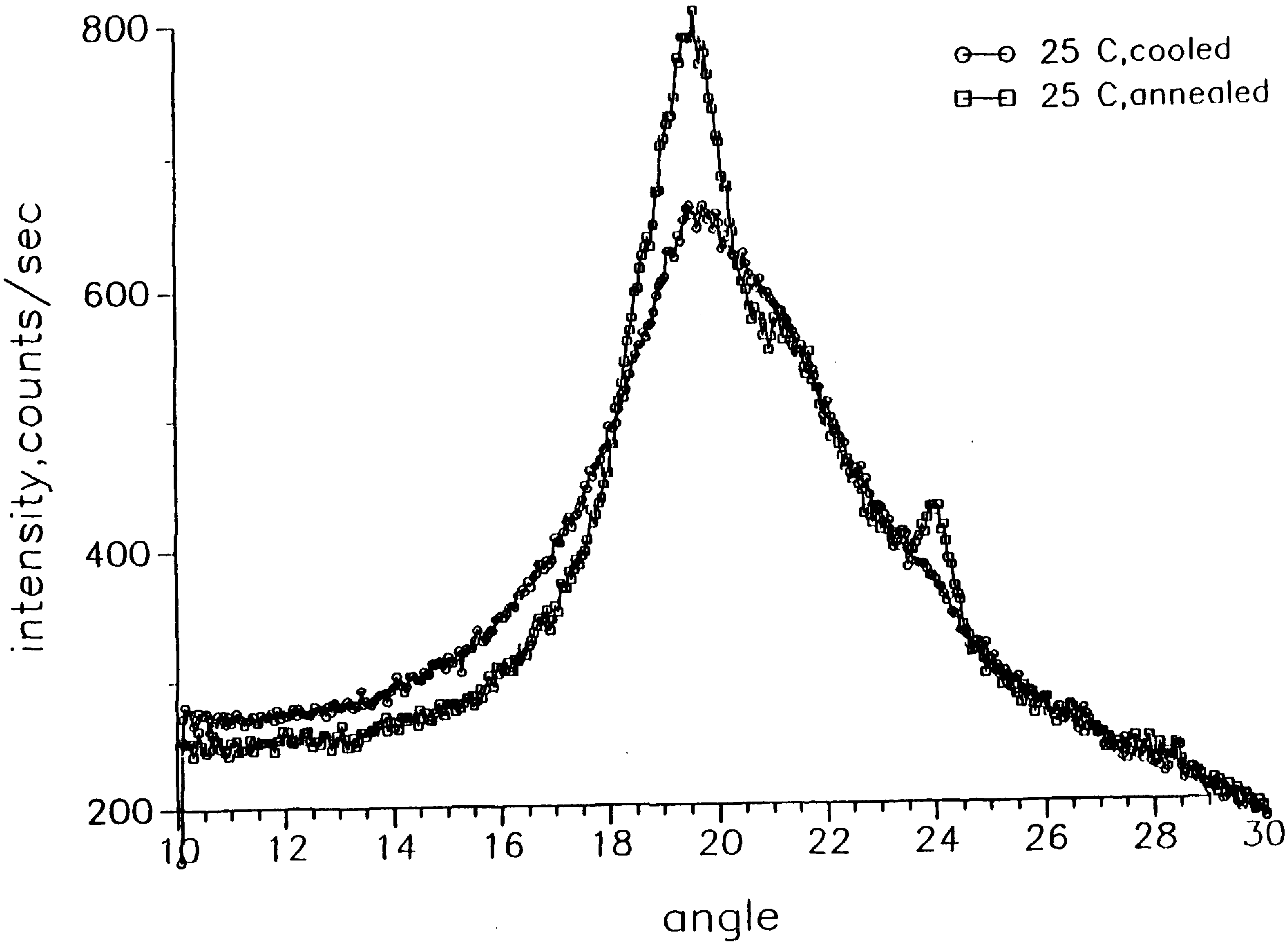
25 C,cooled
25 C,annealed
intensity,counts/sec
800
600
400
200
10
12
14
16
18
20
22
24
26
28
30
angle

Figure 7

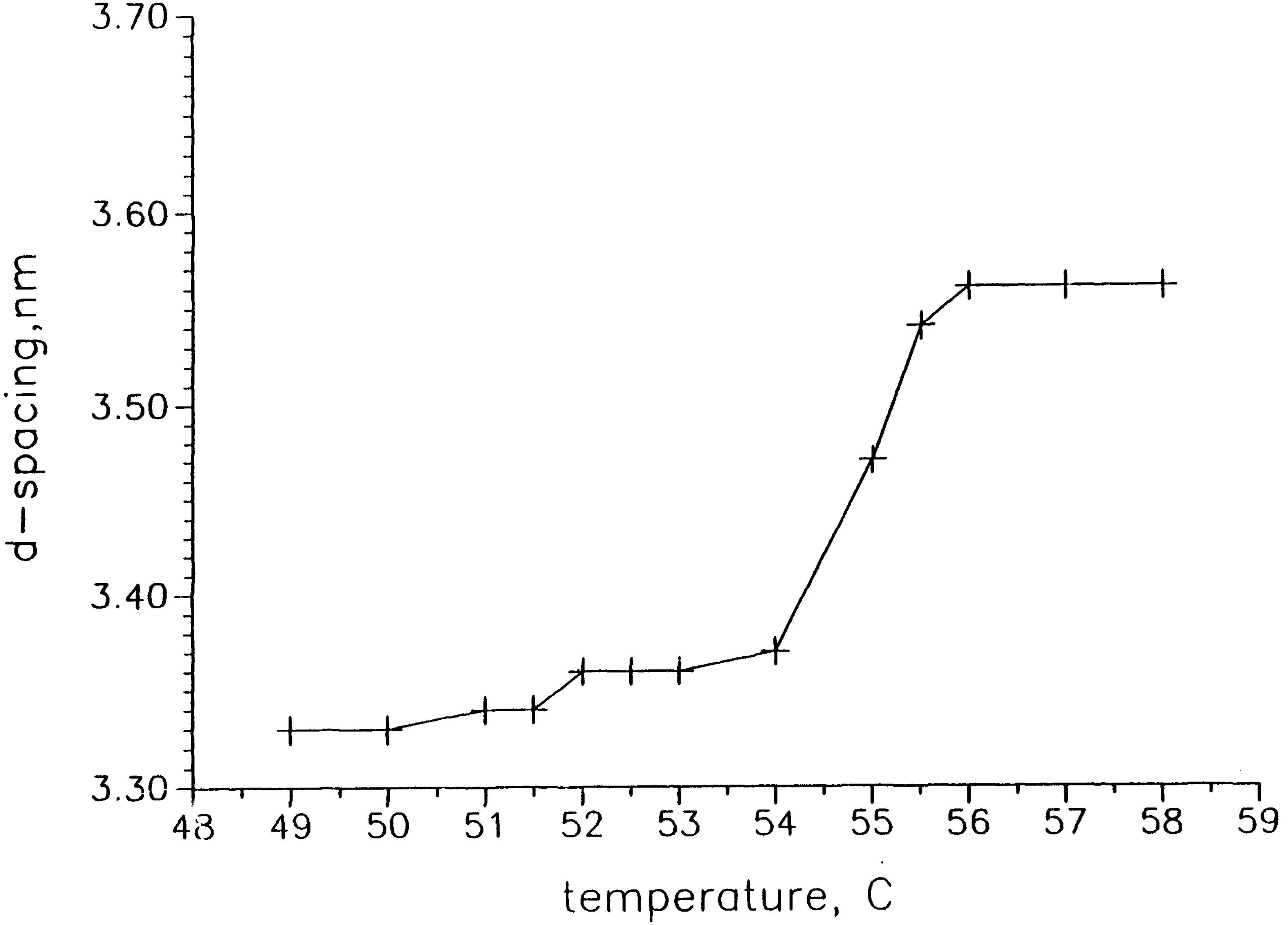
3.70
3.60
3.50
3.40
3.30
d-spacing,nm
48
49
50
51
52
53
54
55
56
57
58
59
temperature, C

Figure 8

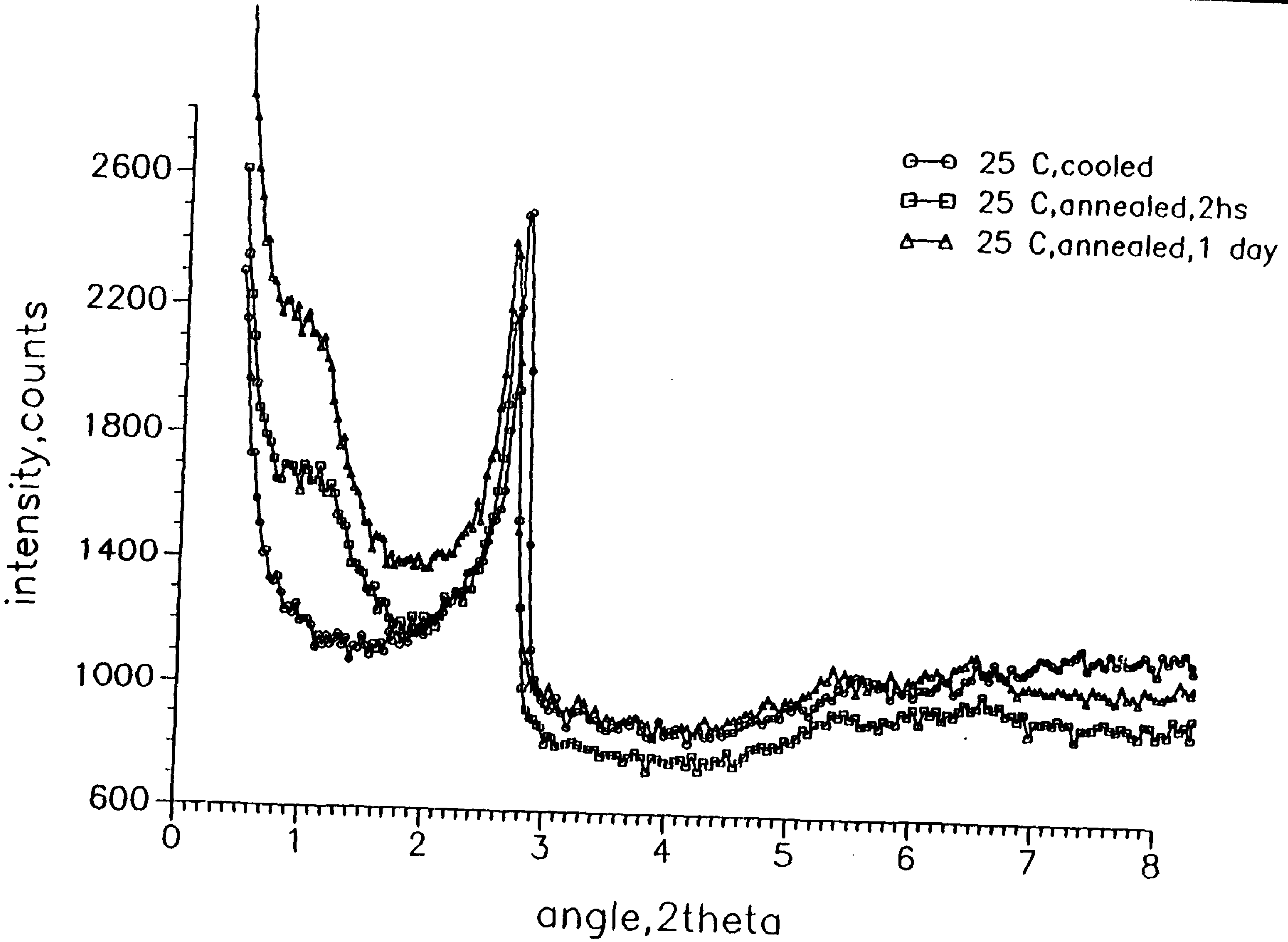

25 C,cooled
25 C,annealed,2hs
25 C,annealed,1 day
intensity,counts
2600
2200
1800
1400
1000
600
0
1
2
3
4
5
6
7
8
angle,2theta

Figure 9